# Short-time particle motion in one and two-dimensional lattices with site disorder $\odot$

Bingyu Cui ■ ; Maxim Sukharev ; Abraham Nitzan



J. Chem. Phys. 158, 164112 (2023) https://doi.org/10.1063/5.0147359





CrossMark

Time to get excited.

Lock-in Amplifiers – from DC to 8.5 GHz









# Short-time particle motion in one and two-dimensional lattices with site disorder

Cite as: J. Chem. Phys. 158, 164112 (2023); doi: 10.1063/5.0147359

Submitted: 21 February 2023 • Accepted: 12 April 2023 •

Published Online: 27 April 2023











# **AFFILIATIONS**

- Department of Chemistry, University of Pennsylvania, Philadelphia, Pennsylvania 19104, USA
- <sup>2</sup>School of Chemistry, Tel Aviv University, Tel Aviv 69978, Israel
- Department of Physics, Arizona State University, Tempe, Arizona 85287, USA
- College of Integrative Sciences and Arts, Arizona State University, Mesa, Arizona 85201, USA
- a) Author to whom correspondence should be addressed: bycui@sas.upenn.edu
- b) E-mail: anitzan@sas.upenn.edu

#### **ABSTRACT**

As in the case of a free particle, the initial growth of a broad (relative to lattice spacing) wavepacket placed on an ordered lattice is slow (its time derivative has zero initial slope), and the spread (root mean square displacement) becomes linear in t at a long time. On a disordered lattice, the growth is inhibited for a long time (Anderson localization). We consider site disorder with nearest-neighbor hopping on one- and two-dimensional systems and show via numerical simulations supported by the analytical study that the short time growth of the particle distribution is faster on the disordered lattice than on the ordered one. Such faster spread takes place on time and length scales that may be relevant to the exciton motion in disordered systems.

Published under an exclusive license by AIP Publishing. https://doi.org/10.1063/5.0147359

### I. INTRODUCTION

Quantum transport in simple dynamic disordered systems has attracted much attention from theorists during the last several decades.<sup>1-5</sup> Under strong disorder, Anderson localization implies that the transport is prohibited beyond a characteristic localization length, with detailed behavior that depends on system dimensionality. 6-12 In a one-dimensional disordered system, Mott and Twose<sup>13</sup> find that all states are exponentially localized, regardless of the amount of disorder, which is later confirmed and extended to two-dimensional systems by Abrahams et al. 14 Such low dimensional disordered systems might range from local site energy disorder in tight-binding models to those with long-range couplings. 15,16 In the case of dynamic disorder that might be induced by the thermal motion of the underlying lattice, short time transport may be faster than in the ordered lattice and becomes diffusive over time so that the mean square displacement scales as  $\langle x^2(t) \rangle \sim t$  when  $t \to \infty$ . Closely related are lattice models that describe quantum diffusion on a linear one-band tight binding lattice with atomic site energies fluctuating in time.1

Generally speaking, the disorder is expected to inhibit transport, as is most critically realized when localization predominates, while dynamic disorder, including thermal effects, is a source of enhanced transport in such systems. The focus of most work on statically disordered systems is the long time localization issue. Here, we draw attention to another aspect of transport in disordered systems: by combining numerical and analytical studies, we show that on a one-dimensional disordered lattice, the short time spread of an initially prepared particle (or exciton) wavepacket is faster than the ballistic growth of the same wavepacket on a perfect monoatomic chain. Numerical studies in two dimensions show similar

An important application of these concepts is found in the field of exciton dynamics.<sup>18</sup> On one hand, exciton transport in static disordered systems is inhibited by localization.  $^{19-21}$  On the other hand, it is assisted by exciton-phonon interaction and becomes diffusive beyond a characteristic coherence length. 20-22 Importantly, decay and recombination imply that considerations of these dynamics are relevant only within the finite exciton lifetime that also determines the so called exciton diffusion length of order ~10-100 nm. 23-26 This implies that in such systems, the early time dynamics investigated here may be more relevant to the observed dynamics than considerations involving disorder-induced localization. To be specific, we use below the language of free exciton propagation on a lattice of two-level emitters. Obviously, the same model is relevant for the motion of non-interacting electrons on a disordered lattice of one-level sites.

The paper is organized as follows. In Sec. II, we introduce the model and describe numerical simulations that demonstrate this behavior. In particular, we find that the disorder-induced excitonspread enhancement results from the destruction of destructive interference that is responsible for the initial slowdown of the wavepacket spread on an ordered lattice. This effect strongly depends on the width of the excitation zone. Excitation spot-sizes as small as 20 nm can be achieved by near field excitation sources,<sup>27</sup> and we find pronounced enhancement for such initial conditions. The effect diminishes for smaller initial excitation spot-sizes and disappears if the exciton is created by a single particle. In Sec. III, we confirm the numerical observation by providing an analytical derivation of the short-time behavior of wavepacket width. Section IV concludes.

## II. NUMERICAL SIMULATIONS

#### A. Model and simulation procedure

We consider a linear chain of two-level emitters with nearestneighbor coupling *J*. The Hamiltonian is

$$\hat{H} = \sum_{n} \epsilon_{n} \hat{c}_{n}^{\dagger} \hat{c}_{n} + J \sum_{n} \left( \hat{c}_{n}^{\dagger} \hat{c}_{n+1} + \hat{c}_{n} \hat{c}_{n+1}^{\dagger} \right), \tag{1}$$

where  $\hat{c}_n^{\dagger}$  and  $\hat{c}_n$ , respectively, create and destroy an excitation on site n, and the coupling I moves it between nearest-neighbor sites. The site energies are sampled from a Gaussian distribution with  $\langle \epsilon_n \rangle_E = 0$ and  $\langle \epsilon_n \epsilon_{n'} \rangle_E = \langle \epsilon_n^2 \rangle_E \delta_{nn'} \equiv \sigma^2 \delta_{nn'}$ . Here,  $\langle \ldots \rangle_E$  denotes the ensemble average, while  $\langle \ldots \rangle$  is used below for the quantum mechanical expectation value. The chain is long enough so that boundary effects are not relevant for the simulated time and length scales. In the reported simulations, we have used emitter chains of  $2.5 \times 10^4$  sites and have ascertained that further increase of the chain length did not affect the computed dynamics. The initial state was taken to be a Gaussian wavepacket with width *D*,

$$\Psi(x, t = 0) = \frac{\sum_{n} e^{-\frac{(na)^{2}}{D^{2}}} \phi(x - na)}{\sqrt{\sum_{n} e^{-2(\frac{na}{D})^{2}}}},$$
 (2)

where  $\phi(x)$  is the orbital wavefunction at position x and a is the lattice spacing, and the site wavefunctions  $\phi(x - na)$  are assumed to be localized at site x = na such that  $\langle \phi(x - na) | f(\hat{x}) | \phi(x - ma) \rangle$ =  $f(x - na)\delta_{nm}$  for an arbitrary function of position f(x), and  $\delta_{nm}$ is the Kronecker delta. In the simulations reported below, the initial values of the Gaussian width were taken to be D = a, 5a, and 20a,which corresponds to an initial wavepacket with  $\langle x^2(t=0)\rangle = \sum_n (na)^2 \exp(-n^2a^2/D^2)/\sum_n \exp(-n^2a^2/D^2)$ . The width at time t is calculated as the square root of  $\langle \delta x^2(t) \rangle \equiv \langle x^2(t) \rangle - \langle x(t) \rangle^2$ , where for any operator  $\hat{A}$ ,

$$\langle A(t)\rangle = \langle \Psi(x, t=0)|e^{i\hat{H}t/\hbar}\hat{A}e^{-i\hat{H}t/\hbar}|\Psi(x, t=0)\rangle. \tag{3}$$

This calculation was repeated over many realizations of the disorder lattice, and the final result was obtained as an ensemble average over the disorder. The time evolution was calculated by diagonalizing the

We consider multiple cases: (1) an ordered system with  $\epsilon_n = 0$ for all n; (2) a system with a static disorder characterized by a Gaussian random distribution of site energies with  $\langle \epsilon_n \rangle_E = 0$  and  $\sigma = \langle \epsilon_n^2 \rangle_E^{1/2}$  ranging between 0.01 and 0.5*J*; (3) for completeness, we also show results for a dynamic disorder model where values of the site energies were resampled at time intervals  $\tau$  that in turn are sampled (unless otherwise stated) from a Poisson distribution characterized by an average renewal time  $\langle \tau \rangle$ . In all simulations, we calculated the width of the wavepacket as a function of time, averaged over trajectories. We have found that averaging over more than 64 trajectories for nearly all simulation parameters does not noticeably change our results.

#### **B.** Numerical results

In an ordered lattice, the time evolution of the root mean square displacement (RMSD) from the origin is similar to the free particle behavior,

$$\sqrt{\langle \delta x^2 \rangle} = \frac{1}{2} \sqrt{D^2 + \frac{\hbar^2 t^2}{4m^2 D^2}},$$

$$\rightarrow \frac{\hbar t}{4mD}, \quad \text{as} \quad t \to \infty,$$
(4)

where the particle mass m is related to the coupling J of Eq. (1) and the lattice constant a by

$$J = \frac{\hbar^2}{2ma^2}. (5)$$

Following an initial time of order  $2mD^2/\hbar$ , in which the wavepacket width increases only slowly, the expansion peaks up and becomes ballistic-like,  $\sqrt{\langle \delta x^2 \rangle} \sim t$  over a long time. The initial incubation period may be discussed in terms of destructive interference between quantum trajectories originating from different sites.

In the simulations described below, unless otherwise noted, the intersite coupling was taken at 0.5 eV, which corresponds to a bandwidth of 1 eV in one dimension. The lattice spacing was a = 1 nm, and the initial excitation spot-size (i.e., the width D of the Gaussian wavepacket) is varied. Excitation spot-sizes as small as ~20 nm<sup>27</sup> can be achieved using near-field excitation sources, and we have simulated processes with smaller initial widths as a way to support the proposed origin of the observed behavior.

Figure 1 shows our results for the increase in the averaged width,

$$\Delta x \equiv \sqrt{\langle \delta x^2(t) \rangle} - \sqrt{\langle \delta x^2(t=0) \rangle}, \tag{6}$$

for several choices of initial wavepacket width D, with different panels displaying results for D/a = 1, 5, and 20 (for the increase in wavepackets of broader widths, see Fig. S1 in the supplementary material). If we accept the picture according to which the slow initial spread reflects destructive interference, this interference appears to erode upon the introduction of site disorder, leading to a significant increase in the spreading rate in this regime. Indeed, when the initial wavepacket width is 20 nm, the expansion rate in the disordered

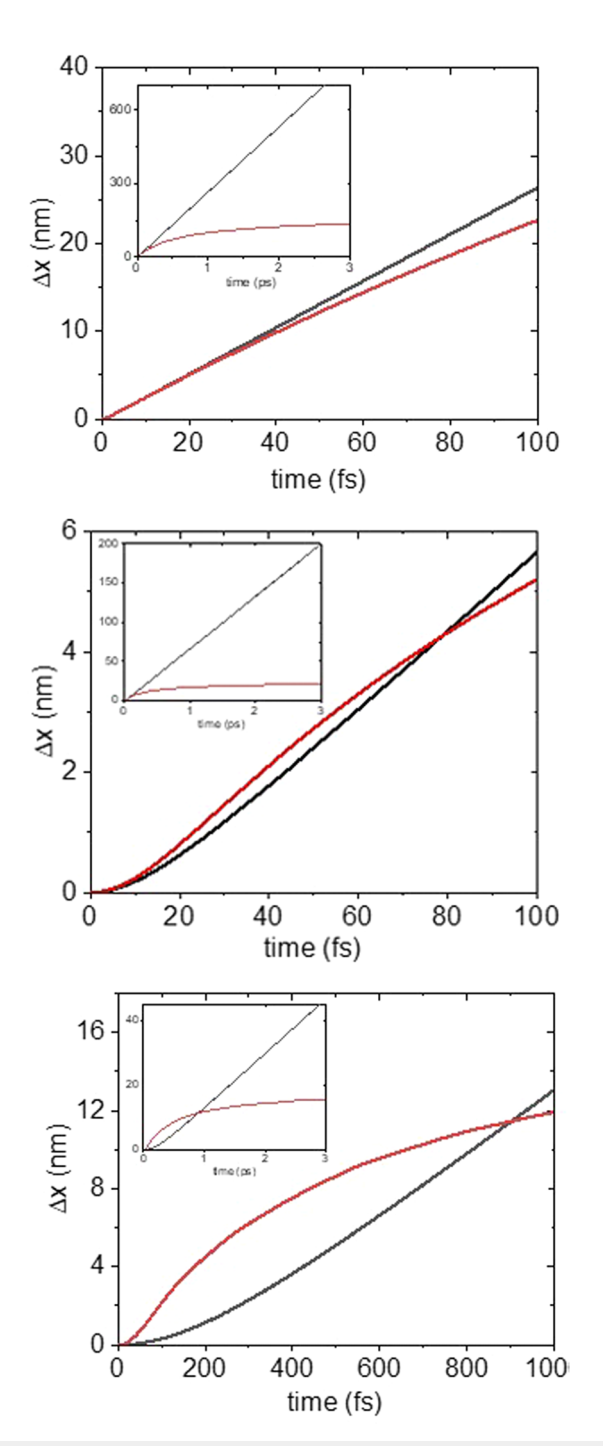


**FIG. 1.** The root mean square displacement Eq. (6) calculated from numerical simulations shows for ordered (black lines) and static disordered (red lines) cases. The hopping parameter is J=0.5 eV, and the disorder parameter is  $\sigma=0.05$  eV. The widths of the initial wavepacket are (a) D=1 nm, (b) 5 nm, and (c) 20 nm. Inset panels are dynamics for a longer time.

systems exceeds that in the ordered lattice until an excess spread of order 10 nm, which is of the order of diffusion lengths of excitons in bulk heterojunction photovoltaic cells. This is a short time effect: in the present one-dimensional site-disordered model with nearestneighbor coupling, all wavefunctions are localized, and expansion eventually stops, as seen in the insets.

Figure 2 displays the dependence of the spread enhancement on the magnitude of the disorder. Two observations can be made. First, the disorder has a larger absolute effect on the spread enhancement for a larger initial wavepacket width, as can be realized by comparing the results of Figs. 1 and 2 (see also Fig. S1). It should be kept in mind, however, that experimental observation of this effect may be easier when the initial excitation spot-size is smaller. Second, the competition between short-time spread enhancement and long-time localization results in the apparent existence of an "optimal" disorder for observing this effect:  $\sigma = 0.03$  eV for the parameters used in Fig. 2. Finally, note that the enhancement can persist through a substantial fraction of typical exciton lifetimes.

A possible explanation of the behavior seen in Fig. 2 is that static disorder has two effects on short-time quantum transport: (a) destroying destructive interference that otherwise inhibits wavepacket propagation, and (b) reducing the effect of coherent transport. The observation that the effect of a smaller disorder amplitude persists longer than that of a larger one implies that removing interference between quantum trajectories initiated on different lattice sites is the more important short time effect, at least for our present choice of parameters.

Our interpretation of the observed effect should not be dimensionality dependent. Indeed, Fig. 3 shows a similar effect in a two-dimensional calculation. In addition, while the Gaussian form of the initial exciton wavepacket is a natural choice for this study, we show (see Fig. S2 in the supplementary material, an initial *p*-like state) that the observed effect does not depend on this choice. These observations suggest that the static disorder can cause enhancement of

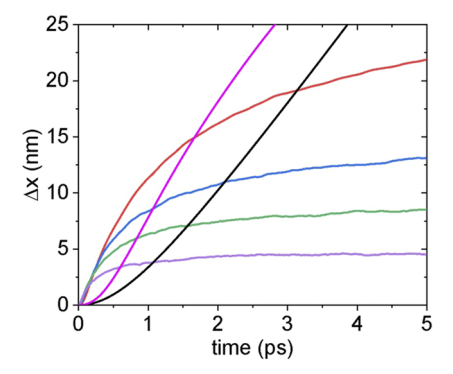


**FIG. 2.** The wavepacket spread  $\Delta x$ , Eq. (6), displayed as a function of time for different magnitudes of the disorder. The initial wavepacket width is D/a=40, and the intersite coupling is 0.05 eV. The black line shows  $\Delta x(t)$  on an ordered lattice, while the purple, green, blue, red, and magenta lines correspond, respectively, to  $\sigma=0.1,0.07,0.05,0.03$ , and 0.005 eV.

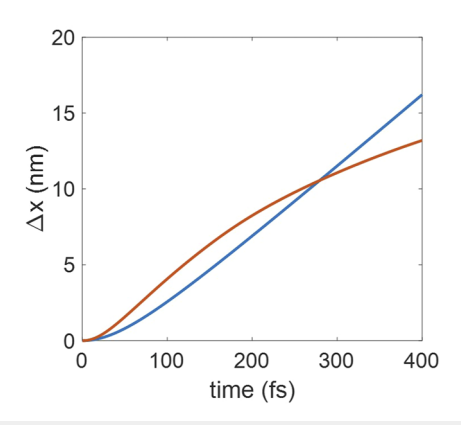


FIG. 3. The root mean square displacement Eq. (6), calculated from numerical simulations in two-dimension, shows ordered (blue line) and static disordered (red line) cases. The hopping parameter is J = 0.5 eV, and the disorder parameter is  $\sigma = 0.1$  eV. The width of the initial wavepacket is D = 10 nm.

exciton diffusion in realistic systems as well, which motivates future studies in this direction.

A direct observation of the predicted short time behavior would require the excitation of a small spot-size and zero linear momentum in the observed direction (as may be achieved by exciting a surface exciton using an incident field normal to the surface). Nevertheless, we have also studied the time evolution of an initially prepared exciton wavepacket with a finite linear momentum, and Fig. S3 in the supplementary material shows the results of such a study. The effect of the initial linear momentum on the spread of the wavepacket appears to be minimal.

As detailed in the introduction, dynamic disorder has long been connected with the acceleration of transport in disordered systems. Recent work on exciton transport has similarly discussed phonon-assisted exciton transport. 18,20,28-30 Figure 4 shows the effect of static and dynamic disorder on carrier mobility in comparison with the underlying ordered lattice. Both the static and dynamic disorders are seen to accelerate the expansion rate of an initially formed wavepacket relative to the disordered system; however, the ballistic dynamics on the ordered lattice takes over after a long time. Expansion under dynamic disorder remains faster than on the ordered lattice for a considerably longer time than that under static order, but given that moving carriers are subjected to competing short time processes (emission and charge separation at nearby interfaces for excitons, recombination, and absorption at surfaces for electrons), the very short time dynamics where static disorder also has a significant effect are relevant to the operation of many such systems.

Finally, we point out that the effect of dynamic disorder has its roots in the properties of the underlying static disorder. This is seen in Fig. 5, which shows the wavepacket expansion process in a system where dynamic disorder is made by a sequence of disorder updates made at constant time intervals  $\tau$ , at which the site energies are resampled from their distribution. Each such update is seen to be followed by the enhanced expansion that subsides as the wavepacket explores its new localization region. Together, these updates lead to a long-time diffusive expansion that reflects the series of transiently accelerated expansions that follow each update.

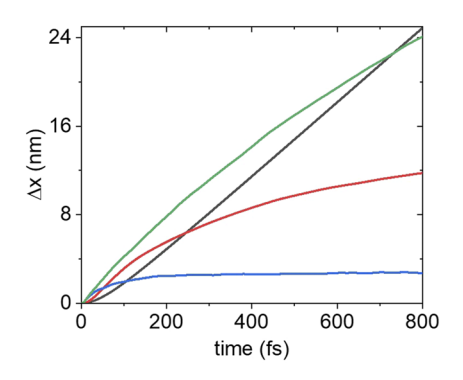


FIG. 4. The root mean square displacement Eq. (6) calculated from numerical simulations shows ordered (black line), static, and dynamic disordered cases. The hopping parameter is J = 0.5 eV, and the disorder parameters are  $\sigma = 0.05$  eV (red line) and  $\sigma$  = 0.2 eV (blue line) for the static disorder and  $\sigma$  = 0.2 eV for the dynamic disorder (green line), in which random renewal kicks are performed at time intervals  $\tau$  sampled from a Poisson distribution with  $\langle \tau \rangle = 52$  fs. The width of the initial wavepacket is D = 10 nm.

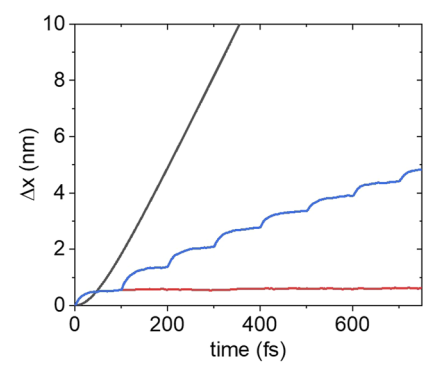


FIG. 5. The root mean square displacement Eq. (6) calculated from numerical simulations shows for ordered (black line), static disordered (red line), and dynamic disordered (blue line; disorder is updated at every  $\tau = 100$  fs) cases. The hopping parameter is J = 0.5 eV, and the disorder parameter is  $\sigma = 0.5$  eV. The width of the initial wavepacket is D = 10 nm.

# III. ANALYTICAL EVALUATION

Here, we attempt to rationalize the main observation made above that the speed of an excitonic wavepacket is initially accelerated by static disorder by looking at the short time evolution under the Hamiltonian (1). Our goal is to calculate the evolution of the mean size  $\Delta x(t)$  of an initially prepared wavepacket for a one-dimensional site-disorder model. In what follows, we describe a short time approximation for this evolution that is able to describe its initial trend.

We start, following Ref. 2, with a more general Hamiltonian given in the site representation by

$$H = \frac{1}{2} \sum_{m,n} \alpha_{mn} \{ |m\rangle \langle n| + |n\rangle \langle m| \} + \frac{1}{2} \sum_{m,n} \beta_{mn} \{ |m\rangle \langle n| + |n\rangle \langle m| \}, \quad (7)$$

where n and m denote sites on a one-dimensional periodic lattice and  $\alpha_{mm}$  and  $\beta_{mn}$  denote the deterministic and random parts, respectively, of the Hamiltonian matrix. Specifically, we assume that Eq. (7) represents an ensemble of identical tight binding systems, each of which is characterized by the tight binding parameter *J*, so that

$$\alpha_{mn} = J\delta_{|m-n|,1},\tag{8}$$

and by a particular realization of the parameters  $\beta_{mn}$ , which we take to be Gaussian random variables specified by the ensemble average  $\langle \beta_{mn} \rangle_E = 0$  and

$$\langle \beta_{mn}\beta_{m'n'}\rangle_E = g(m-n)(\delta_{mm'}\delta_{nn'} + \delta_{mn'}\delta_{m'n} - \delta_{mn}\delta_{m'n'}\delta_{nn'}). \quad (9)$$

Here, g(m-n) measures the strength of the disorder. For thermally induced disorder (i.e., phonons), g reflects the carrier-phonon coupling strength and generally depends on temperature. In particular, we will focus on the case of site-diagonal disorder, as described by  $g(m-n)=g(0)\delta_{mn}$ .

In what follows, we follow the approach of Refs. 2 and 31, adapting it for the short time dynamics under static disorder. The density matrix satisfies the quantum Liouville equation,

$$\frac{\partial \rho}{\partial t} = -\frac{i}{\hbar} [H, \rho], \tag{10}$$

which corresponds to

$$\frac{\partial \rho_{l,r}}{\partial t} = -\frac{i}{\hbar} J(\rho_{l+1,r} + \rho_{l-1,r} - \rho_{l,r+1} - \rho_{l,r-1}) 
- \frac{i}{2\hbar} \sum_{n} \left[ (\beta_{ln} + \beta_{nl}) \rho_{n,r} - (\beta_{nr} + \beta_{rn}) \rho_{l,n} \right].$$
(11)

For convenience, we set the lattice spacing to a = 1. Taking the (spatial) Fourier transformation,  $\tilde{f}(k_1, k_2) = \sum_{lr} e^{-ik_1 l + ik_2 r} f_{l,r}$  on both sides, as well as the ensemble average over the distribution of the  $\beta$ parameters, we obtain

$$\frac{\partial \langle \tilde{\rho}(k_1, k_2; t) \rangle_E}{\partial t} = -\frac{2Ji}{\hbar} (\cos(k_1) - \cos(k_2)) \langle \tilde{\rho}(k_1, k_2; t) \rangle_E$$

$$-\frac{i}{2\pi\hbar} \int_{-\pi}^{\pi} \int_{-\pi}^{\pi} dq dq' \langle \left[ \tilde{\beta}(k_1, q) \delta(q' - k_2) \right]$$

$$-\tilde{\beta}(q', k_2) \delta(q - k_1) \left[ \tilde{\rho}(q, q'; t) \right]_E. \tag{12}$$

The evaluation of a short time solution of Eq. (12) is described in Sec. III of the supplementary material, where details on the way the short time assumption is implemented are provided. This calculation leads, for site diagonal disorder, to the Laplace transform  $\int_0^\infty dt e^{-st} \langle x^2(t) \rangle$  of the RMSD in the form (see Sec. II in the supplementary material for more details),

$$\langle x^2(s) \rangle = - \left[ \frac{\partial^2 \tilde{\chi}(u;s)}{\partial u^2} \right]_{u=0},$$
 (13)

where

$$\tilde{\chi}(u;s) \equiv \frac{1}{2\pi} \int_{-\pi}^{\pi} \langle \hat{R}(p,u;s) \rangle_E dp = \frac{1}{2\pi} \int_{-\pi}^{\pi} \langle \hat{R}(q+p,u;s) \rangle_E dp, \quad (14)$$

and  $\hat{R}(p, u; s) \equiv \hat{p}(k_1, k_2; s)$  with  $k_1 = p + u/2$ ;  $k_2 = p - u/2$ . The function  $\tilde{\chi}(u; s)$  is found (Sec. III in the supplementary material) to be given by

$$\tilde{\chi}(u;s) = \frac{I_1}{1 - 2g(0)I_2/\hbar^2},\tag{15}$$

where  $I_1$  and  $I_2$  are given by

$$I_1(s) = \frac{1}{2\pi} \int_{-\pi}^{\pi} \frac{R(p, u; t = 0) dp}{s - i4J \sin(p) \sin(\frac{u}{2})/\hbar + 2g(0)/(s\hbar^2)},$$
 (16a)

$$I_2(s) = \frac{1}{2\pi} \int_{-\pi}^{\pi} \frac{dp}{s^2 - i4sJ \sin(p) \sin(\frac{u}{2})/\hbar + 2g(0)/\hbar^2}.$$
 (16b)

In Eq. (16), the form R(p, u; t = 0) is obtained from the initial wavepacket, Eq. (2), and is given by

$$R(p, u; t = 0) = \sqrt{2\pi D^2} e^{-\frac{D^2}{4} \left(2p^2 + \frac{u^2}{2}\right)}.$$
 (17)

Finally,  $\langle x^2(t) \rangle$  is calculated as the inverse transform of  $\langle x^2(s) \rangle$ . Figure 6 compares the results obtained from this procedure to those calculated from the numerical simulation (the demonstration on the equivalence of analytical and numerical approaches for ordered lattices is provided in Sec. IV of the supplementary material). While the agreement between these results deteriorates as t increases, the analytical result clearly shows a faster increase in the RMSD for the disordered case in comparison with the ordered system. Note that our approximation [using Eq. (S10) instead of Eq. (S9) in the supplementary material] is rigorously valid only for time shorter than our time unit  $\hbar/J$  (we disregard oscillatory terms that appear on a longer timescale), as indeed seen in the inset of Fig. 6. At longer

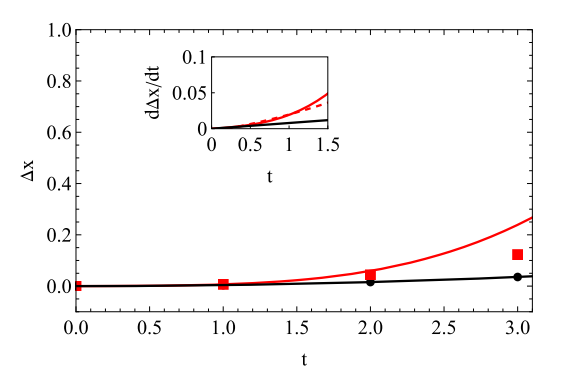


**FIG. 6.** The time evolution of the spread  $\Delta x$  of the exciton wavepacket calculated from Eq. (13) (solid lines) and from our numerical simulation (circles and squares). The initial exciton width is 10. Results of the ordered lattice (g(0) = 0) are shown in solid black lines and circles, while those corresponding to the disordered case  $(g(0) = 0.09J^2)$  are displayed in solid red lines and red squares. The inset shows the time derivative of the change in RMSD, where the red dashed line is the result of the interpolation of numerical dots calculated for the disordered system. The simulation cell contains N = 501 lattice points. An average of n = 60 realizations is taken, and the estimated error in the numerical collection of the disordered system is smaller (<10%) than the size of the point. All numbers are in dimensional units defined in terms of lattice spacing a(=1) and the nearest neighbor coupling energy J(=1) so that the time unit is  $\hbar/J$  (for the choice J=0.5 eV, a unit of time is  $\sim 1.25$  fs. and we take  $\hbar = 1$ ).

times, the analytically calculated spread overestimates the simulation results. This behavior may be viewed as consistent with our assertion that the disorder induced spread enhancement is associated with the erasure of destructive interference, provided that this interference is manifested through the aforementioned oscillations.

#### IV. CONCLUSION

Using one- and two-dimensional site disorder models, we have found that for an initial exciton (or particle) wavepacket whose width encompasses several sites, the initial spread is accelerated by the static disorder. Such disorder affects the time evolution in two ways: first, it disrupts the destructive interference between waves emanating from different sites (hence the initial speed acceleration), and second, it inhibits later coherent evolution (causing later localization). For a broad enough initial wavepacket (as may be formed by optical excitations), the time and length scales of the accelerated speed may be of the order of the excitonic lifetimes and diffusion lengths. Extending the present findings to three-dimensional systems will be the subject of future study.

#### SUPPLEMENTARY MATERIAL

See the supplementary material for examples of the time-dependent spread of a broader choice of wavepacket with different initial widths, an initial wavepacket carrying non-zero momentum, the detailed derivation of the analytical results discussed in Sec. III, and the demonstration that our analytical approach reproduces the exact dynamics in the ordered lattice case.

#### **ACKNOWLEDGMENTS**

This material is based upon work supported by the U.S. National Science Foundation under Grant No. CHE1953701. M.S. is supported by the Air Force Office of Scientific Research under Grant No. FA9550-22-1-0175. We acknowledge Joe Subotnik for many useful discussions.

#### **AUTHOR DECLARATIONS**

#### **Conflict of Interest**

The authors have no conflicts to disclose.

# **Author Contributions**

**Bingyu Cui**: Conceptualization (equal); Formal analysis (equal); Investigation (equal); Methodology (equal); Writing – original draft (equal); Writing – review & editing (equal). **Maxim Sukharev**: Conceptualization (equal); Formal analysis (equal); Investigation (equal); Methodology (equal); Software (equal); Writing – original draft (equal); Writing – review & editing (equal). **Abraham** 

**Nitzan**: Conceptualization (equal); Formal analysis (equal); Investigation (equal); Methodology (equal); Supervision (equal); Writing – original draft (equal); Writing – review & editing (equal).

#### **DATA AVAILABILITY**

The data that support the findings of this study are available within the article and its supplementary material.

#### **REFERENCES**

- <sup>1</sup> A. A. Ovchinnikov and N. S. Erikhman, Zh. Eksp. Teor. Fiz. **67**, 1474 (1974) [Sov. Phys. JETP **40**, 733 (1974)].
- <sup>2</sup> A. Madhukar and W. Post, Phys. Rev. Lett. **39**, 1424 (1977).
- <sup>3</sup> J. Heinrichs, Z. Phys. B: Condens. Matter **50**, 269 (1983).
- <sup>4</sup>Y. Inaba, J. Phys. Soc. Jpn. **50**, 2473 (1981).
- <sup>5</sup>J. Heinrichs, Z. Phys. B: Condens. Matter **52**, 9 (1983).
- <sup>6</sup>P. W. Anderson, Phys. Rev. **109**, 1492 (1958).
- <sup>7</sup>F. Domínguez-Adame and V. A. Malyshev, Am. J. Phys. 72, 226 (2004).
- <sup>8</sup>P. Thiessen, E. Díaz, R. A. Römer, and F. Domínguez-Adame, Phys. Rev. B **95**, 195431 (2017).
- <sup>9</sup>K. J. Kemp, S. Barker, J. Guthrie, B. Hagood, and M. D. Havey, Am. J. Phys. 84, 746 (2016).
- <sup>10</sup> R. Djelti, S. Bentata, Z. Aziz, and A. Besbes, Optik **124**, 3812 (2013).
- <sup>11</sup>D. de Falco and D. Tamascelli, J. Phys. A **46**, 225301 (2013).
- <sup>12</sup> A. Eisfeld, S. M. Vlaming, V. A. Malyshev, and J. Knoester, Phys. Rev. Lett. 105, 137402 (2010).
- <sup>13</sup>N. F. Mott and W. D. Twose, Adv. Phys. **10**, 107 (1961).
- <sup>14</sup>E. Abrahams, P. W. Anderson, D. C. Licciardello, and T. V. Ramakrishnan, Phys. Rev. Lett. 42, 673 (1979).
- <sup>15</sup> A. Rodríguez, V. A. Malyshev, G. Sierra, M. A. Martín-Delgado, J. Rodríguez-Laguna, and F. Domínguez-Adame, Phys. Rev. Lett. **90**, 027404 (2003).
- <sup>16</sup> K. Kawa and P. Machnikowski, Phys. Rev. B **102**, 174203 (2020).
- <sup>17</sup>S. M. Girvin and G. D. Mahan, Phys. Rev. B **20**, 4896 (1979).
- <sup>18</sup>S. J. Jang, *Dynamics of Molecular Excitons* (Elsevier, 2020), pp. 1–20.
- <sup>19</sup> J. Hegarty and M. D. Sturge, J. Opt. Soc. Am. B 2, 1143 (1985).
- <sup>20</sup>W. Barford, Electronic and Optical Properties of Conjugated Polymers (Oxford University Press, 2013), pp. 168–191.
- <sup>21</sup> R. Singh, M. Richter, G. Moody, M. E. Siemens, H. Li, and S. T. Cundiff, Phys. Rev. B **95**, 235307 (2017).
- <sup>22</sup>P. Qi, Y. Luo, B. Shi, W. Li, D. Liu, L. Zheng, Z. Liu, Y. Hou, and Z. Fang, eLight 1. 6 (2021)
- <sup>23</sup>S. M. Menke and R. J. Holmes, Energy Environ. Sci. 7, 499 (2014).
- <sup>24</sup>D. F. Abasto, M. Mohseni, S. Lloyd, and P. Zanardi, Philos. Trans. R. Soc., A 370, 3750 (2012).
- <sup>25</sup>O. V. Mikhnenko, P. W. M. Blom, and T.-Q. Nguyen, Energy Environ. Sci. 8, 1867 (2015).
- <sup>26</sup>Y. Firdaus, V. M. Le Corre, S. Karuthedath, W. Liu, A. Markina, W. Huang, S. Chattopadhyay, M. M. Nahid, M. I. Nugraha, Y. Lin, A. Seitkhan, A. Basu, W. Zhang, I. McCulloch, H. Ade, J. Labram, F. Laquai, D. Andrienko, L. J. A. Koster, and T. D. Anthopoulos, Nat. Commun. 11, 5220 (2020).
- <sup>27</sup>L. Novotny, D. W. Pohl, and B. Hecht, Opt. Lett. **20**, 970 (1995).
- <sup>28</sup> A. Troisi, A. Nitzan, and M. A. Ratner, J. Chem. Phys. **119**, 5782 (2003).
- <sup>29</sup> M. Kilgour and D. Segal, J. Chem. Phys. **143**, 024111 (2015).
- <sup>30</sup>L. Mejía, U. Kleinekathöfer, and I. Franco, J. Chem. Phys. **156**, 094302 (2022).
- <sup>31</sup> N. Singh, "Electronic relaxation and diffusion on dynamically disordered lattices and nanoparticles," Ph.D. thesis, Jawaharlal Nehru University, 2005.